 doi:10.20944/preprints202103.0742.v1

Up regulation in transcript abundance of plastidic isoforms of antioxidant enzymes and accumulation of compatible osmolytes impart tissue tolerance to salinity stressed wheat plants

Lekshmy Sathee*, Raj K Sairam and Viswanathan Chinnusamy

[a]Division of Plant Physiology, Indian Agricultural Research Institute, New Delhi-110012, India

[*]Corresponding author.

E-mail address: lekshmyrnair@gmail.com (Lekshmy Sathee)

Abstract

The response of salt tolerant wheat genotype (Kharchia 65), and sensitive cultivars (HD2687, HD2009, WL711) to vegetative stage salinity stress (for 4 weeks) were studied at 1.1 (control), 9.1 (S1) and 14.2 (S2) dSm^{-1} salinity levels. Based on relative change in Membrane stability, PSII efficiency, retention of chlorophyll and carotenoid contents, Kharchia 65 showed better tolerance to salinity than other genotypes considered. To understand the role of different component mechanisms, expression of genes involved in ion exclusion, antioxidant defence and compatible osmolyte synthesis were analysed. Expression of SOS1 (plasma membrane Na^+/H^+ antiporter), NHX (vacuolar Na^+/H^+ antiporter), Ionic (sodium exclusion) and tissue tolerance (Sodium compartmentation, compatible solute accumulation and antioxidant defence) mechanisms were analysed in leaves of the genotypes after 4 weeks of salinity stress. Expression assay and the content of respective constituents indicated that apart from the well-known ion exclusion ability, Kharchia 65 also showed high level of tissue tolerance resulting in high early vigour and maintenance of growth rate afterwards. In Kharchia 65, sensing of salinity stress at plasma membrane activates NADPH Oxidase (RBOH) genes and generate ROS at apoplast. Apoplastic ROS triggers calcium influx and activates calcium signaling genes of SOS pathway (SOS1 and NHX). ROS generated from organelles chloroplast, peroxisome and mitochondria triggers cellular oxidative burst. ROS and calcium activates MAPK genes and downstream transcription factors, NAC and bZIP. MAPK signaling induces cellular antioxidant and compatible osmolyte biosynthesis and imparts tissue tolerance to salinity.

Keywords: Salinity; wheat; organellar antioxidant; SOS pathway; RBOH

Preprints (www.preprints.org) | NOT PEER-REVIEWED | Posted: 30 March 2021 doi:10.20944/preprints202103.0742.v1

Introduction

Soil salinity is wide-spread in approximately 100 countries around the world with a significant diversity in nature, property and extent of salinisation [1]. The global area of salt-affected soils is around 831 million hectares [2]. A soil is regarded as saline if the electrical conductivity of the soil saturation extract (ECe) surpasses 4 dS m^{-1} [3]. Soil salinity imposes a range of adjustments in plants, viz. alterations in metabolism, nutrient uptake and retardation of growth and development [4]. Despite the well-watered status of soil, salinity induces water deficit by reducing soil water potential making it cumbersome for the roots to extract rhizospheric water [5].

The concomitant water deficit and ion toxicity in saline soils augments generation of cellular reactive oxygen species (ROS) such as superoxide radical (SOR), hydrogen peroxide (H_2O_2), and hydroxyl radical ($OH^{\cdot}$) [6]. As an artefact of photosynthetic electron transport, chloroplasts are oxygen enriched organelles and under stressful situations PSI and PSII become sites of ROS production [7]. The SOR is disimutated to less toxic H_2O_2 by the enzyme superoxide dismutase (SOD). Environmental stresses also promote oxygenase activity of RUBISCO and thus photorespiratory pathway involving chloroplast, peroxisome and mitochondria is activated and generates H_2O_2. ROS are also produced in mitochondria and by plasma membrane bound NADPH oxidase or respiratory burst oxidase homologues (RBOH)in apoplasm. Thus the stress perceived by chloroplast is transmitted to other organelles and result in cellular oxidative burst and the organellar mechanisms to combat ROS are activated [8]. The ROS scavenging system encompasses non-enzymatic and enzymatic antioxidants, such as SODs, catalase (CAT) Ascorbate peroxidase (APX), Glutathione reductase, Ascorbate-glutathione pathway enzymes, ascorbic acid, glutathione, carotenoids, α-tocopherol and polyphenols[7]. Each organelle contains its own antioxidant system, for example MnSOD is located in mitochondria, and peroxisomes, Cu-Zn SOD isoforms are present in cytosol, chloroplast and mitochondria, Fe SOD is found in the chloroplast, APX is located either in thylakoid or cytosol [8] .

Another important adaptation is accumulation of compounds that are osmotically active to reduce cellular osmotic potential and as a scavenger of ROS. Carbohydrates; sucrose, sorbitol, trehalose, mannitol, arabinitol, pinitol, nitrogenous compounds: betaine, proline, aspartate, glycine, glutamate, putrescine, choline, organic acid: malate and oxalate are some of the well-known osmolytes. Proline is a prominent osmolyte synthesised by a two-step pathway, glutamate derived from Glutamate dehydrogenase activity is known to contribute to proline

Preprints (www.preprints.org) | NOT PEER-REVIEWED | Posted: 30 March 2021 doi:10.20944/preprints202103.0742.v1

synthesis. Glycine-betaine is synthesised from choline by a two- step process mediated by the stress regulated enzymes: choline monooxygenase and betaine aldehyde dehydrogenase (BADH) [9–12].

Wheat (*Triticum* spp.) is one of the world's major cereal crop, with the annual worldwide production of over 700million tonnes (http://faostat.fao.org). Both rain-fed and wheat crop is affected by soil salinization [13]. According to CIMMYT reports 8–10 % of the wheat area in India is salinity prone [13]. Majority of Indian salt-tolerant wheat germplasm are derivatives of Kharchia 65, a selection from Kharchi- Pali area of Rajasthan [14]. It is interesting that not much is known about the salt tolerance mechanism of Kharchia 65. Previously our lab has reported that [15] variation in antioxidant activity of subcellular fractions is associated with salinity tolerance in wheat. It was also found that salt tolerant genotypes accumulated higher amount of osmolytes and lesser ROS [16]. Majority of studies on salinity tolerance focusses on ion exclusion trait in wheat, while the information on tolerance to tissue Na^+ i.e., tissue tolerance is highly lacking. A perusal of the foregoing discussion suggests that subcellular antioxidant systems are highly potent for imparting tissue tolerance. The chances of retrograde signalling from organelles to nucleus for transcriptional regulation of antioxidant defence is prominent [7]. The ROS signals from cytosol may be transmitted to nucleus by mitogen-activated protein kinase (MAPK) cascades [8] .Vogel et al [17] reported that MPK6, a regulator of biotic stress signalling plays a role in chloroplast-to-nucleus retrograde signaling. MAPKs are also known to be involved in relaying ROS signals from mitochondria to nucleus. In this study we have analysed the expression dynamics of genes contributing to tissue tolerance and the regulators that are associated with salt tolerance in Kharchia 65.

MATERIALS AND METHODS

Plant material and treatments

Experiments were conducted in p[ot grown plants raised in net house facility, Division of Plant Physiology, Indian Agricultural Research Institute, New Delhi during the *rabi* season. Wheat genotypes viz. Kharchia 65, HD 2009, HD 2687, and WL 711 were raised in earthen pots of uniform size (30 × 30 cm) lined with two layers of 400-gauge polyethylene bags and filled with 10 kg 3:1 ratio mixture of soil: FYM. Seedlings were given salinity treatment with 2.5 litres water (S_0 - control), 100 mM NaCl (S_1) and 200 mM NaCl (S_2) after seven days of

Preprints (www.preprints.org) | NOT PEER-REVIEWED | Posted: 30 March 2021 doi:10.20944/preprints202103.0742.v1

emergence. Scheduled routine of irrigation was practiced for both control and treated pots throughout the crop growth period. Each treatment was replicated 10 times in the form of pots.

Soil samples were collected at weekly intervals from each variety and treatment. From these samples ECe values of soil were estimated, and average of all the values were taken as the mean level of soil salinity. Actual salinity levels expressed as electrical conductivity of soil extract (ECe) were 1.1, 9.1 and 14.2dS m^{-1} for control, 100 and 200 mM NaCl, respectively.

Physiological parameters

Membrane stability index was estimated as described earlier by measuring electrical conductivity of leaf samples incubated at [18] 40 ºC for 30 min (C_1) and after boiling at 100 ºC for 10 min (C_2). Membrane stability index (MSI) was calculated as:MSI = [1 - (C_1/C_2)] x 100.

Chlorophyll (CHL) and carotenoid (CAR) contents were estimated by incubating leaf material in dimethylsulfoxide (DMSO) [19,20] at 65 ºC for 4 h. The absorbance of the extracts were recorded at 470, 645 and 663 nm and was used to calculate the pigment contents.

PSII efficiency was measured by measuring photosynthetic fluorescence using LICOR 6400 IRGA. (LiCOR Ltd., Lincoln, Nebraska, USA) at anthesis stage. Before recording measurement, leaves were covered with black paper to facilitate measurement of maximum fluorescence. Readings were recorded for minimal fluorescence (Fo) and maximum fluorescence (Fm). PS II efficiency = Fv/Fm, Where, Fv = Fm – Fo (Fo: minimal fluorescence, Fm: maximum fluorescence, Fv: variable fluorescence).

Superoxide radical, hydrogen peroxide and TBARS contents estimations

Superoxide radical content was determined by nitroblue tetrazolium chloride (NBT) reduction assay. Hydrogen peroxide was measured as titanium-hydro peroxide complex [21]. The tissue localisation of Superoxide radical, and H_2O_2 were determined as described earlier [22].The lipid peroxidation was measured as thiobarbituric acid reactive substances (TBARS) as described earlier [23]. The membrane injury was also estimated by Evans blue staining followed by spectrophotometric estimation of tissue bound dye [24].

Qualitative estimation of superoxide radicals was done by NBT assay. Localisation of hydrogen peroxide **(**H_2O_2) was determined by DAB assay [25,26]. The second leaf of wheat seedlings was cut into pieces of approx. 1 cm and dipped in NBT/ DAB solution. Leaf segments were viewed under stereomicroscope after removal of chlorophyll from leaf tissue.

Preprints (www.preprints.org) | NOT PEER-REVIEWED | Posted: 30 March 2021 doi:10.20944/preprints202103.0742.v1

Antioxidant enzymes assay

Samples from uppermost expanded leaves were collected from all the treatments and were frozen in liquid N. Frozen samples were extracted using extraction buffer (0.1 M phosphate buffer, pH 7.5, containing 0.5 mM EDTA and 1 mM ascorbic acid). The crude extract filtered through 4 layers of muslin cloth and the filtrate was centrifuged at 4ºC for 20 min at 15,000g. The supernatant was aliquoted and stored in -20ºC freezer [27]. Activity of antioxidant enzymes were assayed using the frozen extract. Total SOD activity was estimated by the inhibition of the photochemical reduction of nitroblue tetrazolium (NBT) by the enzyme [28]. APX was assayed by recording the decrease in optical density due to ascorbic acid at 290 nm [29]. CAT was assayed by measuring the disappearance of H_2O_2 according to Aebi [30]. GR was assayed as per the method of Smith et al. [23].

Estimation of compatible solutes content

For extraction of soluble sugars, dried and powdered leaf samples were boiled with of 80% (v/v) ethanol three times followed by boiling with required amount of distilled water [33]. For estimation of sugars, sample aliquot was mixed anthrone regent and was incubated in a boiling water bath for 8 min. The absorbance of the mixture was recorded at 630 nm after cooling to room temperature in a UV-visible spectrophotometer (model Specord Bio-200, AnalytikJena, Germany).

Trehalose was determined by using the trehalose assay kit from Megazyme (Megazyme International Ltd, Bray, Co. Wicklow, Ireland). Finely ground dry plant material was mechanically shaken with 40 ml of hot (~ 80°C) deionised water on a magnetic stirrer for 15 min. After cooling to room temperature, samples were diluted and filtered. Pre-existing glucose in the filtrate was determined in a control reaction without added trehalase and absorbance was taken at 340nm (A1). Then, the sample was mixed with trehalase, and incubated for 5 min and absorbance was again recorded at 340 nm (A2) against the reagent blank to determine the trehalose content. Difference of A2-A1 was used for obtaining ΔA trehalose (NADPH/2). The concentration of trehalose was determined from the extinction coefficient of NADPH, i.e., 6.3 mM^{-1} cm^{-1}. Trehalose content was obtained by dividing the value of NADPH by 2. Proline content was estimated according to the method of Bates et al. [34]. Glycine-betaine content was estimated according to the protocol of Grieve and Grattan [35].

Assay of enzymes associated with compatible osmolyte biosynthesis

Samples from uppermost expanded leaves were collected from all the treatments and were frozen in liquid N. Frozen samples were extracted using extraction buffer containing 0.1M Na-

Preprints (www.preprints.org) | NOT PEER-REVIEWED | Posted: 30 March 2021 doi:10.20944/preprints202103.0742.v1

citrate, pH 3.7, 1 mM PMSF, 2 mM EDTA and insoluble polyvinylpyrrolidone (10 mg/g dry weight). The homogenate was then filtered through 2 layers of muslin cloth and centrifuged at 31,500g for 30 minutes at 4°C. The supernatant was used for the TPS enzyme assay [36]. Assay mixture contained 0.05 M Hepes–KOH, pH 7.1, 5 mM UDPG, 10 mM glucose 6-phosphate, and 12.5 mM $MgCl_2$, enzyme extract, and water in a total volume of 0.4 ml. Assay mixture was incubated at 35 °C for 30 min; the reaction was stopped by heating at 100°C for 5 min. Thereafter the samples were stored on ice for 10 min and centrifuged at 2000g. UDP formed was determined in the supernatant by the decrease in absorbance at 340 nm in a mixture containing 0.14M Hepes–KOH, pH 7.6, 2 mM phosphoenol pyruvate, 0.3 mM NADH, 5U lactic dehydrogenase, 5U pyruvate kinase, and the sample in a total volume of 0.5 ml. The reaction was started by addition of pyruvate kinase. Controls omitting either glucose-6-phosphate, UDP-glucose or both, were run to eliminate possible interfering reactions, which could produce ADP, UDP or pyruvate. Each determination was made in triplicate. One unit of TPS was defined as the amount of enzyme, which produces 1.0 µmol of NAD^+ per minute at 37 °C and pH 7.0.

For the assay of BADH, plant tissue was homogenized into a fine powder in liquid nitrogen, and then suspended in 10 ml of extraction buffer (50 mM Hepes/KOH pH 8. 0.1 mM EDTA, 5 mM DTT) at room temperature, and centrifuged at 10000g at 4°C for 10 min. Reaction mixture contained 50 mM Hepes/KOH (pH 8.01) 5 mM DTT, 1 mM EDTA, 1 mM betaine aldehyde, 1 mM NAD and 1.0 mg protein from enzyme extract, with a total volume of 1.0 ml [37]. Reaction was carried out at 37 °C for 10 min. Absorbance was recorded in a UV-visible spectrophotometer at 340 nm. One unit of the enzyme activity was defined as the formation of 1 µmol NADH per min under the above condition.

Δ-Pyrroline-5-carboxylate synthetase activity was assayed by recoding the decrease in absorbance due to NADPH at 340 nm [38]. For extraction of enzyme, leaf tissue was ground with liquid nitrogen and in extraction buffer containing 50 mM tris-HCl (pH 7.2), 10 mM $MgCl_2$, 0.6 M KCl, 3 mM EDTA, 1 mM DTT, 5% PVPP and 1 mM β-mercapto ethanol. After grinding, the homogenate was filtered through 2 layers of muslin cloth. The filtrate was then centrifuged at 10000g for 20 minutes at 4 ºC. The supernatant was taken as enzyme extract. Reaction mixture contained 100 mM Tris-HCl (pH 7.2), 25 mM MgCl2, 75 mM sodium glutamate, 5 mM ATP, 0.4 mM NADPH and distilled water to make the volume up to 1 ml. The reaction was started by addition of enzyme extract. The reaction velocity was measured as the rate of consumption of NADPH, monitored as decrease in absorbance at 340 nm as a

Preprints (www.preprints.org) | NOT PEER-REVIEWED | Posted: 30 March 2021 doi:10.20944/preprints202103.0742.v1

function of time. One unit of enzyme activity defined as change in 0.01 O.D. per minute and specific activity as change in O.D. per minute per mg of protein.

Gene expression by RT-PCR

Nucleotide sequences for candidate genes were collected from NCBI using the Basic Local Alignment Search Tool (http://www.ncbi.nlm.nih.gov/BLAST/) [39] to identify the homologs of candidate genes. For RT-PCR expression analysis and cloning of cDNAs, the oligonucleotide primers were designed manually, and oligo quality (to avoid primer dimer, self-dimer etc.), GC % and Tm were analyzed by using Oligoanalyzer 3.0 tool (http://www.idtdna.com/analyzer/Applications/OligoAnalyzer/, Integrated DNA Technologies, Coralville, IA 52241, USA) (Supplementary File1).

For gene expression studies, leaf samples were collected and stored in liquid nitrogen. Total RNA was extracted from leaf tissue of salinity treated and control plants within 24 h of sample collection using RNAeasy plant minikit (Qiagen Inc., Chatsworth CA 91311, USA, Cat No: 749040) according to the manufacturer's instruction. DNA contamination was removed from the RNA samples using DNase I (Qiagen Science, Maryland, USA). One µg of total RNA was reverse transcribed using Qiagen one-step RT-PCR kit. PCR conditions were standardized using gene-specific primers for *actin*. Reactions were conducted using QN 96 Thermal cycler (Quanta biotech, England), under the following conditions: initial PCR activation step: 15 min at 95 ^{o}C, reverse transcription: 30 min at 50 ^{o}C, denaturation: 1 min at 94 ^{o}C, annealing: 1 min at 57 ^{o}C, extension: 1 min at 72 ^{o}C, final extension: 10 min at 72 ^{o}C. Linear amplification for semi-quantitative RT-PCR was obtained with 27 cycles. The amplification products were electrophoresed on 1.2 % agarose gel at 120 volts in TBE buffer (0.4M Tris – borate, 0.001 M EDTA, pH 8.0) using known concentration DNA ladders. Gels were stained with ethidium bromide and visualized on Uvi Pro Gel Documentation system (Uvitec, England) (Supplementray File 2-3).

cDNA sequencing

RT-PCR amplified cDNAs were fractionated on agarose gel and purified. The purified cDNAs for each gene were cloned into pTz57R/T vector and transformed into *Escherichia coli* (strain DH5α) cells. DH5α cells transformed with recombinant plasmids were selected based on antibiotic resistance as well as α-complementation method. Ampicillin resistant putative recombinants were selected for further analysis. Plasmids were isolated from the confirmed colonies and restriction analysis was carried out by using *Kpn I* and *Hind III* enzymes flanking

Preprints (www.preprints.org) | NOT PEER-REVIEWED | Posted: 30 March 2021 doi:10.20944/preprints202103.0742.v1

the cloning site of the vector, to confirm the presence of cloned insert cDNA. *E. coli* cells containing desired recombinant plasmid were given to Xcelris Labs Limited, Bodakdev, Ahmedabad, India, for sequencing the cloned insert cDNA. The sequences were analysed for specifivity of amplicons and were submitted to NCBI (Supplementary file 4) the sequences were used to design qPCR primers (Supplementary file 5).

Gene expression by qRT-PCR

Leaf tissues were sampled in liquid nitrogen for RNA extraction. High quality total RNA was extracted using QIAGEN RNeasy® plant mini kit followed by DNase I treatment to obtain DNA free RNA. RNA was quantified using thermo nanodrop 2000c spectrophotometer. First strand cDNA was synthesized from 1 µg of total RNA by using Superscript–III reverse transcriptase (Invitrogen, USA). To study the expression level of candidate genes, qRT-PCR was carried using Power SYBR® Green Master Mix (Applied Biosystems, USA) on real time PCR detection system (Applied Biosystems). qRT-PCR was done using gene specific primers for MAPK6, bZIP6, NAC4, SOS1 and NHX1 and genes encoding antioxidant and osmolyte metabolism (Supplementary file 3). Melt curve data collection and analysis was enabled and qRT-PCR products were also visualised by agarose gel electrophoresis to confirm the single specific band. Normalization of the data for each transcript was carried out using *TaActin* as an internal control and level of expression were analyzed using 2^{-DDCt} method [40].

Statistical analyses

Values are means of 3 observations (n = 3), and data was subjected to analysis of variance by CRD. F-test was carried out to test the significance of the treatment differences and the least significant differences (LSD) were computed to test the significance of the different treatments at 5% level of probability by the SPSS 16.0. Mean separation was done using Sidak's multiple comparisons test following one-way ANOVA. Graphs and heatmaps were made using MS Excel and GraphPad Prism version 8 (La Jolla, California, USA).

RESULTS

Salinity stress negatively affects physiological parameters

Salinity stress imposition decreased the total chlorophyll and carotenoid content of all genotypes, The relative reduction in pigments was less in Kharchia 65 (Fig 1a, b). Stress induced injury was more pronounced in genotypes WL 711 and HD2687, HD 2009 showed only a moderate drop in chlorophyll content. There was decline in MSI with increase in salinity

Preprints (www.preprints.org) | NOT PEER-REVIEWED | Posted: 30 March 2021 doi:10.20944/preprints202103.0742.v1

in all the four genotypes (Fig.1c) with a lower average decline in Kharchia 65 than in other genotypes. Results on photosystem II efficiency is presented in Fig. 1d Photosystem II efficiency showed reduction in all the genotypes under salinity treatment.

Variation in ROS accumulation and associated enzymes

Exposure to soil salinity significantly increased the H_2O_2 accumulation in all the genotypes than that that observed in control (Fig. 2a, b). Kharchia 65 showed lowest H_2O_2 content under salinity treatment, whereas HD 2009, HD 2687 and WL 711 recorded had more than 2 fold increase over control in S2 treatment. Tolerant genotype Kharchia 65 maintained significantly less increase in SOR content, recording an increase of 10-14 % over control, where as HD 2009, HD 2687 and WL 711 showed significant increase of 128, 136 and 98.8 % over control in S2 treatment (Fig. 2c, d) Subjecting wheat plants to different salinity levels resulted in significant increase in TBARS contents in all the genotypes (Fig. 2e). Maximum increase was found in HD2687 (139%) and WL 711 (165%) under S2 treatment. Membrane injury visualized by Evans blue staining was also in agreement with ROS accumulation. Kharchia 65 showed lowest membrane injury in both S1 and S2 treatments.

Activity of SOD was increased under salinity stress (Fig. 3a), Kharchia 65 had higher levels of SOD activity under S1 and S2 treatments. HD 2009 also maintained higher salinity induced SOD activity, whereas, HD 2687 and WL 711 showed significantly less SOD activity at S2. Significant increase in ascorbate peroxidase (APX) activity was noticed under both the levels of salinity in all the genotypes (Fig. 3b), the magnitude of increase was much higher in Kharchia 65, followed by HD 2009. Salinity stress resulted in increase in catalase (CAT) activity in all the genotypes (Fig. 3c). There was noticeable increase in CAT and GR activity by salinity in all the genotypes. HD 2009 also maintained significantly higher CAT activity under both salinity levels. WL 711 and HD 2687 showed the lesser salinity induced increase in catalase activity. Glutathione reductase (GR) activity increased under salinity treatment in all the genotypes (Fig. 3d). Kharchia 65 manifested higher GR activity in all the treatments.

Variation in osmolyte accumulation and associated enzymes

Total soluble sugar content escalated under salinity treatments noticeably in all the genotypes (Fig. 4a). Sugar accumulation was highest in S_1 treatment in all the genotypes. Sugar content was significantly higher in Kharchia 65 under S_1 and S_2 salinity levels, while lowest content was observed in HD 2687. Trehalose content (Fig. 4b) increased with the increase in salinity treatments in all the genotypes and Kharchia 65 showed 6 and 8 folds increases in

Preprints (www.preprints.org) | NOT PEER-REVIEWED | Posted: 30 March 2021 doi:10.20944/preprints202103.0742.v1

trehalose content under S_1 and S_2 salinity levels, respectively. Glycine-betaine content was also augmented by salinity in all the genotypes (Fig. 4c). In S_1 treatment all the genotypes showed significant increase, however, highest content was observed in Kharchia 65. Under S_2 treatment, only Kharchia 65 maintained significantly higher stress induced glycine-betaine content and all other genotypes showed decline over S_1 treatment. Proline content (Fig. 4d) increased in all the four genotypes with increasing salinity levels. Significantly greater increases in proline content were observed in HD 2009 and HD 2687 than Kharchia 65, and lowest in WL 711 under both the salinity levels. The increases were 5.71, 6.97, 6.07 and 4.78; 6.59, 7.84, 6.72 and 5.69 times over control in case of Kharchia 65, HD 2009, HD 2687 and WL 711 under S_1 and S_2 treatments, respectively at vegetative stage.

Stress induced up regulation in the TPS activity in all the genotypes was greater under S_1 treatment (Fig. 5a). Under S_2 treatment, TPS activity declined compared to S_1 treatment, though remaining higher than the control values in case of Kharchia 65 and HD 2009, while in case of HD 2687 and WL 711 the decline was below the control level. Salinity treatment led to an increase in betaine aldehyde dehydrogenase (BADH) activity in all the genotypes; the greater increases were observed under S_2 treatment (Fig. 5b). Kharchia 65, followed by HD 2009 showed significantly higher BADH activity. Δ-Pyrroline-5-carboxylate synthetase activity (Fig. 5c) increased in all the genotypes under S_1 and S_2 treatments, highest activity was observed in HD 2009 and HD 2687, followed by Kharchia 65 and WL 711.

Transcript abundance of ROS and Osmolyte metabolic enzymes and cDNA sequencing

RT-PCR for antioxidant enzymes and osmolyte biosynthesis enzymes were performed with gene specific primers and amplicons were obtained in all the four genotypes under all the three treatments (Supplementary File 3-4). Complete/ partial CDS of the antioxidant enzymes are and osmolyte biosynthesis enzymes are registered in NCBI data base and is presented in Supplementary File 5. The cloned cDNA sequences were used to design gene specific qPCR primers and qPCR validation of expression data is presented in Fig 6a, b.

For *Cu-ZnSODc* Kharchia 65 showed very little expression under control as well as S1 and S2. Other genotypes like HD 2009, HD 2687 and WL 711 showed salinity induced over expression. More intense band was found under S1 treatment in HD 2009. Complete coding sequences for *Cu-ZnSODc* of Kharchia 65, HD 2009, HD 2687 and WL 711 have been registered in NCBI data base vide GenBank Acc. Nos. JQ269674.1, JQ269675.1, JQ269676.1 and JQ269677.1 respectively (Supplementary File 3, Fig 6a, b). In the case of plastidic Cu/Zn-superoxide dismutase (Cu/Zn-SODp) gene, Kharchia 65 showed very high salinity induced

Preprints (www.preprints.org) | NOT PEER-REVIEWED | Posted: 30 March 2021 doi:10.20944/preprints202103.0742.v1

expression under both S1 and S2 treatments. But all other genotypes showed decrease in transcript abundance of this gene under both S1 and S2 treatments. HD 2009 performed comparatively better than WL 711 and HD 2687 (Supplementary File 3, Fig 6a, b). Partial nucleotide sequences for *Cu-ZnSODp* of Kharchia 65, HD 2009, HD 2687 and WL 711 have been registered in NCBI data base vide GenBank Acc. Nos. JQ269670.1, JQ269671.1, JQ269672.1 and JQ269673.1 respectively.

In the case of chloroplastic iron superoxide dismutase (Fe-SOD) gene, RT-PCR amplicons of size 520 bp were amplified from the four genotypes. Only Kharchia 65 maintained transcript abundance of of Fe SOD in S1 and S2. All other genotypes were having very low expression especially in S2 treatment (Supplementary File 3, Fig 6a, b). Partial nucleotide sequences for FeSOD of Kharchia 65, HD 2009, HD 2687 and WL 711 have been registered in NCBI data base vide GenBank Acc. Nos. JQ269678.1, JQ269679.1, JQ269680.1 and JQ269681.1 respectively.

In the case of mitochondrial Mn-superoxide dismutase (Mn-SOD) gene, RT-PCR amplicons of size 473 bp were amplified from the four genotypes. Expression was more or less similar in all genotypes under all treatments (Supplementary File 3, Fig 6a, b). Slight increase in expression was found in Kharchia 65 and HD 2009 under S1 and S2 treatments. Partial nucleotide sequences for MnSOD of Kharchia 65, HD 2009, HD 2687 and WL 711 have been registered in NCBI data base vide GenBank Acc. Nos. JQ230558.1, JQ230559.1, JQ230560.1 and JQ230561.1 respectively.

In the case of thylakoid bound ascorbate peroxidase (APX) gene, RT-PCR amplicons of size 652 bp were amplified from the four genotypes. Kharchia 65 showed very high salinity induced over expression under both S1 and S2 treatments. HD 2009 performed comparatively better than WL 711 and HD 2687. HD 2687 showed decrease in transcript abundance of this gene under both S1 and S2 (Supplementary File 3, Fig 6a, b). WL 711 showed slight expression only in the case of S1 treatment. Partial nucleotide sequences for APX of Kharchia 65, HD 2009, HD 2687 and WL 711 have been registered in NCBI data base vide GenBank Acc. Nos. JQ230566.1, JQ230567.1, JQ230568.1 and JQ230569.1 respectively. In the case of catalase (CAT) gene RT-PCR amplicons of size 752 bp were amplified from the four genotypes.. Salinity led to over expression of CAT in Kharchia 65 and HD 2009 only in S1 treatment. Under S2 only Kharchia 65 showed expression of the gene. Partial nucleotide sequences for CAT of Kharchia 65, HD 2009, HD 2687 and WL 711 have been registered in NCBI data base vide GenBank Acc. Nos. JQ230562.1, JQ230563.1, JQ230564.1 and JQ230565.1 respectively.

Preprints (www.preprints.org) | NOT PEER-REVIEWED | Posted: 30 March 2021 doi:10.20944/preprints202103.0742.v1

RT-PCR for osmolyte biosynthesis enzymes were performed with gene specific primers and amplicons were obtained in all the four genotypes under all the three treatments (Supplementary Fig 4). In the case of TPS gene, RT-PCR amplicons of size 590 bp were amplified from the four genotypes. Very little expression was observed in control plants of all the four genotypes (Supplementary File 4, Fig 6a, b). Salinity induced over expression was observed in all the four genotypes. However, under S_1 and S_2 treatments very prominent bands were observed only in tolerant genotype Kharchia 65. Partial cDNA sequences of *T6PS* of 597, 597, 591 and 591 bp were obtained in case of Kharchia 65, HD 2009, HD 2687 and WL 711, respectively. Partial nucleotides sequences of Kharchia 65, HD 2009, HD 2687 and WL 711 have been registered in NCBI data base vide GenBank ID: JQ073558.1, **J**Q073559, JQ073560 and JQ073561 respectively. In the case of *TPP* gene, RT-PCR amplicons of size 630 bp were amplified from the four genotypes. Very little expression was observed in control plants of the four genotypes. Salinity induced over expression was observed in all the four genotypes, however, very prominent bands were observed in tolerant genotype Kharchia 65 and HD 2009 under both S1 and S_2 treatments (Supplementary File 4, Fig 6a, b). In HD 2687 there was moderate up regulation under S_1 but not under S_2. In contrast WL 711 showed significant up regulation only under S_2 treatment. Partial cDNA sequences of *TPP* of 633, 633, 632 and 632 bp were obtained in case of Kharchia 65, HD 2009, HD 2687 and WL 711, respectively. GenBank ID: JQ073562, JQ073563, JQ073564 and JQ073565, respectively. In the case of *betaine aldehyde dehydrogenase* (*BADH*) gene, RT-PCR was performed with gene specific primers and expected amplicons of the size 680 bp were obtained for all the four genotypes under all the three treatments. Salinity induced upregulated expression was prominent only in the case of Kharchia 65 and HD 2009 under both S_1 and S_2 treatments (Supplementary File 4, Fig 6a, b). Band intensity in Kharchia 65 was more than HD 2009 under both S_1 and S_2 treatments. Partial cDNA sequences of *BADH* of 682 bp were obtained in case of Kharchia 65, HD 2009, HD 2687 and WL 711. GenBank ID: JQ269661, JQ269662, JQ269663 and JQ269664, respectively.

In the case of *P5CS* gene, RT-PCR amplicons of size 680 bp were amplified from the four genotypes. Unlike genes of other osmolytes, *P5CS* expression in Kharchia 65 was less than HD 2009 and HD 2687 under both S_1 and S_2 treatments. Very little expression was observed in WL 711 under both S_1 and S_2 treatments compared to the other three genotypes. Partial cDNA sequences of *P5CS* of 678, 674, 667 and 669 bp were obtained in case of Kharchia 65, HD 2009, HD 2687 and WL 711, respectively. GenBank ID: JQ063079, JQ063080, JQ063081 and JQ063081, respectively (Supplementary File 4-5, Fig 6a, b).

Preprints (www.preprints.org) | NOT PEER-REVIEWED | Posted: 30 March 2021 doi:10.20944/preprints202103.0742.v1

qRT-PCR analysis of genes associated with tissue tolerance and stress signaling

Genes associated with tissue tolerance and stress signaling were analyzed by qPCR. The genes associated with sodium exclusion (SOS1) and Vacuolar partitioning (NHX) were both upregulated by salinity. As the intensity of salinity was increased from S1 to S2, expression of the genes was also upregulated. Expression of RBOH-F gene was upregulated by salinity stress. In S2 treatment there was approximately 5-10-fold upregulation in expression (Fig 6a, b). The relative expression of *MAPK* gene was increased by both S1 and S2 treatments. Maximum upregulation was observed in Kharchia 65, followed by other genotypes (Fig 6a, b). Expression of stress regulated transcription factors, bZIP and NAC were also upregulated by salinity stress in all the genotypes. NAC4 expression in S2 treatment was significantly different among all the genotypes, while in the case of bZIP, Kharchia 65 maintained the highest stress induced expression in S2 treatment.

DISCUSSION

The present study unveiled that salinity stress negatively affects various physiological traits in wheat. The tolerant cultivar Kharchia 65 performed better in terms of various parameters. Sairam and Srivastava [41] used membrane stability index (MSI) to differentiate wheat genotypes differing in salinity tolerance. Salinity driven decrease in MSI [5,16] is reported in wheat and maize plants. MSI showed a positive association with osmotic potential, cellular K^+ concentration, capacity of osmotic adjustment, water contents in salinity stressed plants [42]. Leaf injury can be measured by various methods, ranging from leaf disc leakage to chlorophyll fluorescence. This study revealed that the dark-adapted fluorescence parameter Fv/Fm ratio was a relatively sensitive index of salt injury as PSII efficiency was found to decrease more in salinity stressed susceptible plants, whereas tolerant genotypes like Kharchia 65 had slight decrease in PSII efficiency under salinity stress.

The genotypic difference in retention of chlorophyll and carotenoid contents might be due to tissue level mechanisms, which resisted pigment degradation in tolerant genotypes than susceptible ones. These effects could an indicator of better tissue tolerance and the resultant favorable cellular and membrane ultrastructure. Tissue tolerance represents the capability of tissues to remain physiologically active despite the presence of high tissue ion concentration [43]. Osmotic adjustment in halophytic plants is achieved by retention of Na^+ and Cl^- in leaves and roots of cells is essential for plants to survive salinity. Accumulation is an energy-efficient osmotic adjustment. The adverse the ions are circumvented, leading to ‘tissue tolerance’.

Preprints (www.preprints.org) | NOT PEER-REVIEWED | Posted: 30 March 2021 doi:10.20944/preprints202103.0742.v1

According to Munns et al [44], for identifying genotypes with tissue tolerance, screening methods should focus on osmotic adjustment (ion and organic solute based) and understanding tissue mechanisms to tolerate excess ions.

An important observation under salinity stress is the generation of various ROS, especially SOR and H_2O_2, leading to membrane lipid peroxidation and injury. The tolerant genotype Kharchia 65 and the moderately tolerant HD 2009 showed lower abundance of ROS in comparison to susceptible genotypes HD 2687 and WL 711. Salt induced oxidative stress has also been reported in other crop plants [5,45]. Ashraf and McNeilly [46] found a positive correlation between the activities of antioxidant enzymes and salt tolerance in *Brassica napus.* Gene expression studies indicated that plastidic forms of Cu/Zn-SOD and Fe-SOD, and ascorbate peroxidase were significantly upregulated in tolerant genotypes. Shalata et al. [47] reported the importance of organellar antioxidant system in salinity tolerance of tomato. Hernandez et al. [48] found a positive association of antioxidant defence gene expression and salt tolerance in pea. In our study Mn-SOD did not show significant over expression under salinity treatment. It has been previously reported that Mn-SOD is involved in scavenging superoxide radicals produced during monocarpic senescence in maize [50]. There was significantly higher expression of CAT, FeSOD and Plastidic Cu/Zn-SOD in Kharchia 65, resulting in reduced levels of oxidative stress. Sairam and Srivastava [16]reported that susceptibility of wheat genotype to long term salinity stress was due to relatively lesser induction of SOD isozymes resulting in higher oxidative stress in the form of H_2O_2 and TBARS. It is also notable that different isoforms of a same antioxidant enzyme have different activities in lines/cultivars differing in salt tolerance. For example, enhanced activities of both Mn-SOD and Cu/Zn- SOD were recorded in the mitochondria of the leaves of salt sensitive pea plants. In contrast, enhanced activity of Mn-SOD was found in the mitochondria of salt tolerant pea plants due to salt stress [49]. Under severe salinity stress (S_2 treatment) SOD and APX activities and gene expression were found to be decreased. Hernandez et al. [48] reported that when K^+ availability is below optimal, Na^+ inhibits the activity of Mn-SOD and CuZn-SOD in cowpea protoplasts.

Surplus accumulation of sucrose and/or reducing sugars in cytosol contributes to turgor maintenance of cells facing osmotic stress [51]. Plastidic starch reserve is promptly converted to sucrose along with concomitant inhibition of starch synthesis [52]. Total soluble sugar content was highest in salinity stressed wheat plants. Kharchia 65 showed a greater upsurge in TSS under S1 and S2 treatments. Salinity induced surge in trehalose concentration was reported

Preprints (www.preprints.org) | NOT PEER-REVIEWED | Posted: 30 March 2021 doi:10.20944/preprints202103.0742.v1

wheat [53] and rice [54]. There was a significant up-regulation of TPS enzyme activity and *TPS* and *TPP* gene expression in tolerant cv. Kharchia 65. Enhanced activity of TPS enzyme has also been reported by Bashiti et al. [53] in salinity stressed wheat plants. Trehalose-6-phosphate is dephosphorylated into trehalose by the enzyme trehalose-6-phosphate phosphatase (TPP). Lopez et al [55]also reported the effect of salinity on both TPP and TPS enzymes in *Lotus japonicus*. Transgenic tobacco plants over-expressing the *Escherichia coli TPS* gene exhibited enhanced rates of photosynthesis per unit leaf area (Paul et al., 2001), enumerating the importance of trehalose metabolism in plants. In this study we are reporting for the first time that salinity induced transcriptional up-regulation of *T6PS* and *TPP* genes in wheat genotypes is associated with increased TPP activity and trehalose synthesis.

There was sharp increase in glycine-betaine content in Kharchia 65 under increasing salt stress. The role of glycine-betaine as osmoprotectant has been established from ling time [5,16]. Glycine-betaine preserves thylakoid and plasma membrane integrity after exposure to saline solutions or temperature extremes [56]. In higher plants betaine aldehyde dehydrogenase (BADH) is a key enzyme, which catalyses the conversion of betaine-aldehyde to glycine-betaine [57]. The in BADH activity and *BADH* gene expression showed a positive correlation in salinity stressed wheat plants. In sugar beet the BADH activity increased 2–4-fold in leaves and roots as NaCl was increased from 0 to 500 mM, and the increase in BADH activity was correlated with the level of *BADH* mRNA [58].

It is well established that proline accumulates in plants during adaptation to various types of environmental stresses, such as salinity and drought [59,60]. Proline content was increased by salinity stress in wheat genotypes, the magnitude of increase was highest in HD 2009 (moderately tolerant) and HD 2687 (susceptible), than in salinity tolerant genotype Kharchia 65. The transcriptional activation of *P5CS*, encoding the rate-limiting enzyme in the proline biosynthetic pathway [61,62] was correlated to proline content, in wheat. It speculated that Kharchia 65 might have achieved stress acclimation much earlier than HD 2009 and HD 2687 and used proline as a source of energy and nitrogen, hence leading to low level of proline content, P5CS activity and gene expression.

We analysed the dynamics of genes contributing to tissue tolerance and the signalling by qPCR. In agreement with our previous report, the sodium exclusion and partitioning genes SOS1 and NHX were upregulated by salt stress. A scrutiny of the above-mentioned details proposes that subcellular antioxidant systems and compatible solutes are extremely important for imparting tissue tolerance. Retrograde signalling from organelles to

Preprints (www.preprints.org) | NOT PEER-REVIEWED | Posted: 30 March 2021 doi:10.20944/preprints202103.0742.v1

nucleus is important for transcriptional regulation of tissue tolerance traits [7]. The ROS signals from cytosol, chloroplast and mitochondria may be relayed to nucleus by MAPK signalling [8], as reported by Vogel et al [17] about MPK6 as a key player of chloroplast-to-nucleus retrograde signaling. NADPH-dependent oxidase complexes are are membrane ROS producing machinery also called as the RBOHs [63]. RBOH catalyzes the electron transfer from NADPH to molecular oxygen and the SOR generated is then converted to H_2O_2 by spontaneous reaction or by SODs [64,65]. Expression of RBOH-F gene was up-regulated by salinity stress and more so in the tolerant genotype. We found upregulation of *TaMAPK* gene in leaves of wheat genotypes. Kharchia 65, which is having better antioxidant defense system and is more tolerant to salinity stress, also maintained higher relative expression of *MAPK* gene. The cytosolic ROS burst is indispensable for ROS-elimination by it's crosstalk with ABA mediated stress signalling. ABA signalling can initiate phosphorylation of the target bZIP TFs by a MAPK, a CDPK or by CKIIs. At the translational level, specific cross talks exist between the activated bZIP TF and other bZIP TFs or NAC TF. The activated bZIP TF initiates transcription of the target genes (ROS and Osmolyte homeostasis) and alleviate stress induced damage. Our results show that *TabZIP1* was upregulated only in tolerant genotype Kharchia 65. Over-expression of *CAbZIP1* conferred drought and salt tolerance to *Arabidopsis* transgenic plants. Zhang *et al.* [66] reported that the expression of *TabZIP1* was induced by salt, low temperature, and wounding treatments. Thus *TabZIP1* may be a key player in wheat's response to various environmental stresses. The underlying molecular mechanisms can be complicated as the expression of *TabZIP1* was maximum at 2 h and 24 h after treatment with ABA [66]. Several transcriptomic studies have revealed that many of the *NAC* genes are controlled by diverse biotic and abiotic stresses, suggesting that they have vital role in stress signaling. Our results revealed that salinity treatment also upregulated *TaNAC* gene expression in in leaves of wheat genotypes. Xia *et al.* [67] reported that the *TaNAC8* transcript abundance was up-regulated by salt stress, osmotic stress (PEG treatment) and low-temperature treatment, suggesting the role of *TaNAC8* in responses to these environmental stresses.

Conclusion

Salinity induced ROS production has been suggested as the primary cause for stress induced damages to nucleic acids, proteins lipids and pigments. The results of the present investigation suggest that under salinity stressed condition, Kharchia 65 behaved differently than other genotypes like HD 2687 and WL 711. Genotype Kharchia 65 manifested salt tolerance depicted as retention of chlorophyll and carotenoids, reduced abundance of oxidative

stress indicators, higher accumulation of osmolytes. The stress protective antioxidant enzymes and osmolyte biosynthesis enzymes were more active due to transcriptional activation of the corresponding genes. The perusal of results and the previous information suggests that in Kharchia 65, sensing of salinity stress at plasma membrane activates NADPH Oxidase (RBOH) genes and generate ROS at apoplast. Apoplastic ROS triggers calcium influx and activates calcium signaling genes of SOS pathway (SOS1 and NHX). ROS generated from organelles chloroplast, peroxisome and mitochondria triggers cellular oxidative burst. ROS and calcium activates MAPK genes and downstream transcription factors, NAC and bZIP. MAPK signaling induces cellular antioxidant and compatible osmolyte biosynthesis and imparts tissue tolerance to salinity. AtSOS1 interacts with Radical induced cell death 1 (RCD1) a regulator of oxidative-stress signaling and establishes a crosstalk between the ionic and oxidative-stress adaptation. It can thus be speculated that in salinity tolerant genotypes, ROS burst mediated triggering of putative RCDs [68] and calcium signaling improves sodium exclusion (by activating SOS1) and tissue tolerance mechanisms: vacuolar sodium compartmentation (by NHX1) osmolyte accumulation and antioxidant defense. (Fig 7).

Acknowledgements

Authors are thankful to the ICAR-Indian Agricultural Research Institute for funding and providing the necessary facilities. LS acknowledge CSIR- Junior research fellowship support received during the course of the study. Authors also acknowledge the financial support received from NAHEP-CAAST, ICAR-IARI (Grant No. NAHEP/CAAST/2018-19/07).

Author contributions

L.S. conducted the experiments and wrote the manuscript. RKS, VC and LS designed the experiments, contributed resources and finalised the manuscript.

Competing interests

The authors declare no competing interests.

References

1. Munns, R.; Tester, M. Mechanisms of salinity tolerance. *Annu. Rev. Plant Biol.* 2008, *59*, 651–681.

2. Rengasamy, P. World salinization with emphasis on Australia. *J. Exp. Bot.* **2006**, *57*, 1017–1023, doi:10.1093/jxb/erj108.

3. Chhabra, R. Classification of salt-affected soils. *Arid L. Res. Manag.* **2005**, *19*, 61–79, doi:10.1080/15324980590887344.

4. MUNNS, R. Physiological processes limiting plant growth in saline soils: some dogmas and hypotheses. *Plant. Cell Environ.* **1993**, *16*, 15–24, doi:10.1111/j.1365-3040.1993.tb00840.x.

5. Kholová, J.; Sairam, R.K.; Meena, R.C.; Srivastava, G.C. Response of maize genotypes to salinity stress in relation to osmolytes and metal-ions contents, oxidative stress and antioxidant enzymes activity. *Biol. Plant.* **2009**, *53*, 249–256, doi:10.1007/s10535-009-0047-6.

6. Puniran-Hartley, N.; Hartley, J.; Shabala, L.; Shabala, S. Salinity-induced accumulation of organic osmolytes in barley and wheat leaves correlates with increased oxidative stress tolerance: In planta evidence for cross-tolerance. *Plant Physiol. Biochem.* **2014**, *83*, 32–39, doi:10.1016/j.plaphy.2014.07.005.

7. Noctor, G.; Reichheld, J.; Foyer, C. ROS-related redox regulation and signaling in plants. *Semin Cell Dev Biol 80*, 3–12.

8. Noctor, G.; Foyer, C.H. Intracellular redox compartmentation and ROS-related communication in regulation and signaling. *Plant Physiol.* **2016**, *171*, 1581–1592, doi:10.1104/pp.16.00346.

9. Tuteja, N. *Mechanisms of High Salinity Tolerance in Plants*; Elsevier Masson SAS, 2007; Vol. 428; ISBN 9780123739216.

10. Rai, V.K. Role of amino acids in plant responses to stresses. *Biol. Plant.* 2002, *45*, 481–487.

11. Hayat, S.; Hayat, Q.; Alyemeni, M.N.; Wani, A.S.; Pichtel, J.; Ahmad, A. Role of proline under changing environments: A review. *Plant Signal. Behav.* 2012, *7*.

12. Munns, R.; Tester, M. Mechanisms of salinity tolerance. *Annu Rev Plant Biol* **2008**, *59*.

13. Mujeeb-Kazi, A.; De Leon, J.L.D. Conventional and alien genetic diversity for salt tolerant wheats: focus on current status and new germplasm development. In; Springer, Dordrecht, 2002; pp. 69–82.

14. Rana, R. Evaluation and utilisation of traditionally grown cereal cultivars on salt affected areas in India. *Indian J. Genet. Plant Breed.* **1986**, *46*, 121–135.

15. Sairam, R.K.; Dharmar, K.; Chinnusamy, V.; Lekshmy, S.; Joshi, R.; Bhattacharya, P. The role of non-symbiotic haemoglobin and nitric oxide homeostasis in waterlogging tolerance in Vigna species. *Biol. Plant.* **2012**, *56*, 528–536, doi:10.1007/s10535-012-0064-8.

16. Sairam, R.K.; Rao, K.; Srivastava, G.C. Differential response of wheat genotypes to long term salinity stress in relation to oxidative stress, antioxidant activity and osmolyte concentration. *Plant Sci.* **2002**, *163*, 1037–1046, doi:10.1016/S0168-9452(02)00278-9.

17. Vogel, M.O.; Moore, M.; König, K.; Pecher, P.; Alsharafa, K.; Lee, J.; Dietz, K.J. Fast retrograde signaling in response to high light involves metabolite export, MITOGEN-ACTIVATED PROTEIN KINASE6, and AP2/ERF transcription factors in Arabidopsis. *Plant Cell* **2014**, *26*, 1151–1165, doi:10.1105/tpc.113.121061.

18. Sairam, R.K.; Deshmukh, P.S.; Shukla, D.S. Tolerance of drought and temperature stress in relation to increased antioxidant enzyme activity in wheat. *J. Agron. Crop Sci.* **1997**, *178*, 171–178, doi:10.1111/j.1439-037X.1997.tb00486.x.

19. Hiscox, J.D.; Israelstam, G.F. A method for the extraction of chlorophyll from leaf tissue without maceration. *Can. J. Bot.* **1979**, *57*, 1332–1334, doi:10.1139/b79-163.

20. Arnon, D.I. COPPER ENZYMES IN ISOLATED CHLOROPLASTS. POLYPHENOLOXIDASE IN BETA VULGARIS . *Plant Physiol.* **1949**, *24*, 1–15, doi:10.1104/pp.24.1.1.

21. Rao, M. V.; Paliyath, G.; Ormrod, D.P.; Murr, D.P.; Watkins, C.B. Influence of salicylic acid on H2O2 production, oxidative stress, and H2O2-metabolizing enzymes. Salicylic acid-mediated oxidative damage requires H2O2. *Plant Physiol.* **1997**, *115*, 137–149, doi:10.1104/pp.115.1.137.

22. Padhan, B.K.; Sathee, L.; Meena, H.S.; Adavi, S.B. CO 2 Elevation Accelerates Phenology and Alters Carbon / Nitrogen Metabolism vis-à-vis ROS Abundance in Bread Wheat. **2020**, *11*, 1–18, doi:10.3389/fpls.2020.01061.

23. Heath, R.L.; Packer, L. Photoperoxidation in isolated chloroplasts. I. Kinetics and stoichiometry of fatty acid peroxidation. *Arch. Biochem. Biophys.* **1968**, *125*, 189–198, doi:10.1016/0003-9861(68)90654-1.

24. Kato, Y.; Miura, E.; Matsushima, R.; Sakamoto, W. White leaf sectors in yellow variegated2 are formed by viable cells with undifferentiated plastids. *Plant Physiol.* **2007**, *144*, 952–960, doi:10.1104/pp.107.099002.

25. Kumar, D.; Yusuf, M.; Singh, P.; Sardar, M.; Sarin, N. Histochemical Detection of

Superoxide and H2O2 Accumulation in Brassica juncea Seedlings. *BIO-PROTOCOL* **2014**, *4*, doi:10.21769/bioprotoc.1108.

26. Padhan, B.K.; Sathee, L.; Meena, H.S.; Adavi, S.B.; Jha, S.K.; Chinnusamy, V. CO2 Elevation Accelerates Phenology and Alters Carbon/Nitrogen Metabolism vis-à-vis ROS Abundance in Bread Wheat. *Front. Plant Sci.* **2020**, *11*, doi:10.3389/fpls.2020.01061.

27. Sairam, R.K.; Dharmar, K.; Lekshmy, S.; Chinnusamy, V. Expression of antioxidant defense genes in mung bean (Vigna radiata L.) roots under water-logging is associated with hypoxia tolerance. *Acta Physiol. Plant.* **2011**, *33*, 735–744, doi:10.1007/s11738-010-0598-3.

28. DHINDSA, R.S.; PLUMB-DHINDSA, P.; THORPE, T.A. Leaf Senescence: Correlated with Increased Levels of Membrane Permeability and Lipid Peroxidation, and Decreased Levels of Superoxide Dismutase and Catalase. *J. Exp. Bot.* **1981**, *32*, 93–101, doi:10.1093/jxb/32.1.93.

29. Y Nakano, K.A. Hydrogen peroxide is scavenged by ascorbate specific peroxidase in spinach chloroplasts. *Plant Cell Physiol* **1981**, *22*, 867–880.

30. Aebi, H. [13] Catalase in Vitro. *Methods Enzymol.* **1984**, *105*, 121–126, doi:10.1016/S0076-6879(84)05016-3.

31. Smith, I.K.; Vierheller, T.L.; Thorne, C.A. Assay of glutathione reductase in crude tissue homogenates using 5,5′-dithiobis(2-nitrobenzoic acid). *Anal. Biochem.* **1988**, *175*, 408–413, doi:10.1016/0003-2697(88)90564-7.

32. Mhamdi, A.; Noctor, G.; Baker, A. Plant catalases: Peroxisomal redox guardians. *Arch. Biochem. Biophys.* 2012, *525*, 181–194.

33. McCready, R.M.; Guggolz, J.; Silviera, V.; Owens, H.S. Determination of Starch and Amylose in Vegetables. *Anal. Chem.* **1950**, *22*, 1156–1158, doi:10.1021/ac60045a016.

34. Bates, L.S.; Waldren, R.P.; Teare, I.D. Rapid determination of free proline for water-stress studies. *Plant Soil* **1973**, *39*, 205–207, doi:10.1007/BF00018060.

35. Grattan, S.R.; Grieve, C.M. Salinity-mineral nutrient relations in horticultural crops. *Sci. Hortic. (Amsterdam).* 1998, *78*, 127–157.

36. Errey, J.C.; Lee, S.S.; Gibson, R.R.; Fleites, C.M.; Barry, C.S.; Jung, P.M.J.; O'Sullivan, A.C.; Davis, B.G.; Davies, G.J. Mechanistic insight into enzymatic glycosyl transfer with retention of configuration through analysis of glycomimetic inhibitors. *Angew. Chemie - Int. Ed.* **2010**, *49*, 1234–1237, doi:10.1002/anie.200905096.

37. Guo, Y.; Zhang, L.; Xiao, G.; Cao, S.; Gu, D.; Tian, W.; Chen, S. Expression of betaine aldehyde dehydrogenase gene and salinity tolerance in rice transeenic plants. *Sci. China, Ser. C Life Sci.* **1997**, *40*, 496–501, doi:10.1007/BF03183588.

38. García-Ríos, M.; Fujita, T.; Larosa, P.C.; Locy, R.D.; Clithero, J.M.; Bressan, R.A.; Csonka, L.N. Cloning of a polycistronic cDNA from tomato encoding γ-glutamyl kinase and γ-glutamyl phosphate reductase. *Proc. Natl. Acad. Sci. U. S. A.* **1997**, *94*, 8249–8254, doi:10.1073/pnas.94.15.8249.

39. Altschul, S.F.; Madden, T.L.; Schäffer, A.A.; Zhang, J.; Zhang, Z.; Miller, W.; Lipman, D.J. Gapped BLAST and PSI-BLAST: A new generation of protein database search programs. *Nucleic Acids Res.* 1997, *25*, 3389–3402.

40. Livak, K.J.; Schmittgen, T.D. Analysis of Relative Gene Expression Data Using Real-Time Quantitative PCR and the 2 C T Method. *METHODS* **2001**, *25*, 402–408, doi:10.1006/meth.2001.1262.

41. Sairam, R.K.; Srivastava, G.C. Changes in antioxidant activity in sub-cellular fractions of tolerant and susceptible wheat genotypes in response to long term salt stress. *Plant Sci.* **2002**, *162*, 897–904, doi:10.1016/S0168-9452(02)00037-7.

42. Munns, R. Comparative physiology of salt and water stress. *Plant, Cell Environ.* **2002**, *25*, 239–250, doi:10.1046/j.0016-8025.2001.00808.x.

43. Munns, R.; Passioura, J.B.; Colmer, T.D.; Byrt, C.S. Osmotic adjustment and energy limitations to plant growth in saline soil. *New Phytol.* **2020**, *225*, 1091–1096, doi:10.1111/nph.15862.

44. Munns, R.; Gilliham, M. Salinity tolerance of crops - what is the cost? *New Phytol.* 2015, *208*, 668–673.

45. Yeo, A.R.; Lee, À.S.; Izard, P.; Boursier, P.J.; Flowers, T.J. Short- and long-term effects of salinity on leaf growth in rice (Oryza sativa L.). *J. Exp. Bot.* **1991**, *42*, 881–

889, doi:10.1093/jxb/42.7.881.

46. Ashraf, M.; McNeilly, T. Responses of four Brassica species to sodium chloride. *Environ. Exp. Bot.* **1990**, *30*, 475–487, doi:10.1016/0098-8472(90)90028-3.

47. Shalata, A.; Mittova, V.; Volokita, M.; Guy, M.; Tal, M. Response of the cultivated tomato and its wild salt-tolerant relative Lycopersicon pennellii to salt-dependent oxidative stress: The root antioxidative system. *Physiol. Plant.* **2001**, *112*, 487–494, doi:10.1034/j.1399-3054.2001.1120405.x.

48. Hernández, J.A.; Jiménez, A.; Mullineaux, P.; Sevilia, F. Tolerance of pea (*Pisum sativum L.*) to long-term salt stress is associated with induction of antioxidant defences. *Plant. Cell Environ.* **2000**, *23*, 853–862, doi:10.1046/j.1365-3040.2000.00602.x.

49. Jiménez, A.; Hernández, J.A.; Del Río, L.A.; Sevilla, F. Evidence for the presence of the ascorbate-glutathione cycle in mitochondria and peroxisomes of pea leaves. *Plant Physiol.* **1997**, *114*, 275–284, doi:10.1104/pp.114.1.275.

50. Prochazkova, D.; Sairam, R.K.; Srivastava, G.C.; Singh, D. V. Oxidative stress and antioxidant activity as the basis of senescence in maize leaves. *Plant Sci.* **2001**, *161*, 765–771, doi:10.1016/S0168-9452(01)00462-9.

51. Mahajan, S.; Tuteja, N. Cold, salinity and drought stresses: An overview. *Arch. Biochem. Biophys.* **2005**, *444*, 139–158, doi:10.1016/j.abb.2005.10.018.

52. Kumutha, D.; Sairam, R.K.; Ezhilmathi, K.; Chinnusamy, V.; Meena, R.C. Effect of waterlogging on carbohydrate metabolism in pigeon pea (Cajanus cajan L.): Upregulation of sucrose synthase and alcohol dehydrogenase. *Plant Sci.* **2008**, *175*, 706–716, doi:10.1016/j.plantsci.2008.07.013.

53. El-Bashiti, T.; Hamamci, H.; Öktem, H.A.; Yücel, M. Biochemical analysis of trehalose and its metabolizing enzymes in wheat under abiotic stress conditions. *Plant Sci.* **2005**, *169*, 47–54, doi:10.1016/j.plantsci.2005.02.024.

54. Garg, A.K.; Kim, J.K.; Owens, T.G.; Ranwala, A.P.; Do Choi, Y.; Kochian, L. V.; Wu, R.J. Trehalose accumulation in rice plants confers high tolerance levels to different abiotic stresses. *Proc. Natl. Acad. Sci. U. S. A.* **2002**, *99*, 15898–15903, doi:10.1073/pnas.252637799.

55. López, M.; Herrera-Cervera, J.A.; Lluch, C.; Tejera, N.A. Trehalose metabolism in root nodules of the model legume Lotus japonicus in response to salt stress. *Physiol. Plant.* **2006**, *128*, 701–709, doi:10.1111/j.1399-3054.2006.00802.x.

56. Chen, T.H.H.; Murata, N. Enhancement of tolerance of abiotic stress by metabolic engineering of betaines and other compatible solutes. *Curr. Opin. Plant Biol.* 2002, *5*, 250–257.

57. Yang, C.; Chong, J.; Li, C.; Kim, C.; Shi, D.; Wang, D. Osmotic adjustment and ion balance traits of an alkali resistant halophyte Kochia sieversiana during adaptation to salt and alkali conditions. *Plant Soil* **2007**, *294*, 263–276, doi:10.1007/s11104-007-9251-3.

58. Lv, X.; Chen, S.; Wang, Y. Advances in Understanding the Physiological and Molecular Responses of Sugar Beet to Salt Stress. *Front. Plant Sci.* 2019, *10*.

59. Parida, A.K.; Dagaonkar, V.S.; Phalak, M.S.; Aurangabadkar, L.P. Differential responses of the enzymes involved in proline biosynthesis and degradation in drought tolerant and sensitive cotton genotypes during drought stress and recovery. *Acta Physiol. Plant.* **2008**, *30*, 619–627, doi:10.1007/s11738-008-0157-3.

60. Mbarki, S.; Skalicky, M.; Vachova, P.; Hajihashemi, S.; Jouini, L.; Zivcak, M.; Tlustos, P.; Brestic, M.; Hejnak, V.; Khelil, A.Z. Comparing salt tolerance at seedling and germination stages in local populations of medicago ciliaris l. To medicago intertexta l. and medicago scutellata l. *Plants* **2020**, *9*, doi:10.3390/plants9040526.

61. Silva-Ortega, C.O.; Ochoa-Alfaro, A.E.; Reyes-Agüero, J.A.; Aguado-Santacruz, G.A.; Jiménez-Bremont, J.F. Salt stress increases the expression of p5cs gene and induces proline accumulation in cactus pear. *Plant Physiol. Biochem.* **2008**, *46*, 82–92, doi:10.1016/j.plaphy.2007.10.011.

62. Dudziak, K.; Zapalska, M.; Börner, A.; Szczerba, H.; Kowalczyk, K.; Nowak, M. Analysis of wheat gene expression related to the oxidative stress response and signal transduction under short-term osmotic stress. *Sci. Rep.* **2019**, *9*, doi:10.1038/s41598-019-39154-w.

63. Suzuki, N.; Miller, G.; Morales, J.; Shulaev, V.; Torres, M.A.; Mittler, R. Respiratory burst oxidases: The engines of ROS signaling. *Curr. Opin. Plant Biol.* 2011, *14*, 691–

699.

64. Sairam, R.K.; Dharmar, K.; Chinnusamy, V.; Lekshmy, S.; Joshi, R.; Bhattacharya, P. NADPH oxidase as the source of ROS produced under waterlogging in roots of mung bean. *Biol. Plant.* **2011**, *55*, 741–746, doi:10.1007/s10535-011-0179-3.

65. Zhou, J.; Xia, X.J.; Zhou, Y.H.; Shi, K.; Chen, Z.; Yu, J.Q. RBOH1 -dependent H2O2 production and subsequent activation of MPK1/2 play an important role in acclimation-induced cross-tolerance in tomato. *J. Exp. Bot.* **2014**, *65*, 595–607, doi:10.1093/jxb/ert404.

66. Zhang, Y.; Zhang, G.; Xia, N.; Wang, X.J.; Huang, L.L.; Kang, Z.S. Cloning and characterization of a bZIP transcription factor gene in wheat and its expression in response to stripe rust pathogen infection and abiotic stresses. *Physiol. Mol. Plant Pathol.* **2008**, *73*, 88–94, doi:10.1016/j.pmpp.2009.02.002.

67. Xia, N.; Zhang, G.; Sun, Y.F.; Zhu, L.; Xu, L.S.; Chen, X.M.; Liu, B.; Yu, Y.T.; Wang, X.J.; Huang, L.L.; et al. TaNAC8, a novel NAC transcription factor gene in wheat, responds to stripe rust pathogen infection and abiotic stresses. *Physiol. Mol. Plant Pathol.* **2010**, *74*, 394–402, doi:10.1016/j.pmpp.2010.06.005.

68. Katiyar-Agarwal, S.; Jin, H. Role of Small RNAs in Host-Microbe Interactions. *Annu. Rev. Phytopathol.* **2010**, *48*, 225–246, doi:10.1146/annurev-phyto-073009-114457.

Preprints (www.preprints.org) | NOT PEER-REVIEWED | Posted: 30 March 2021 doi:10.20944/preprints202103.0742.v1

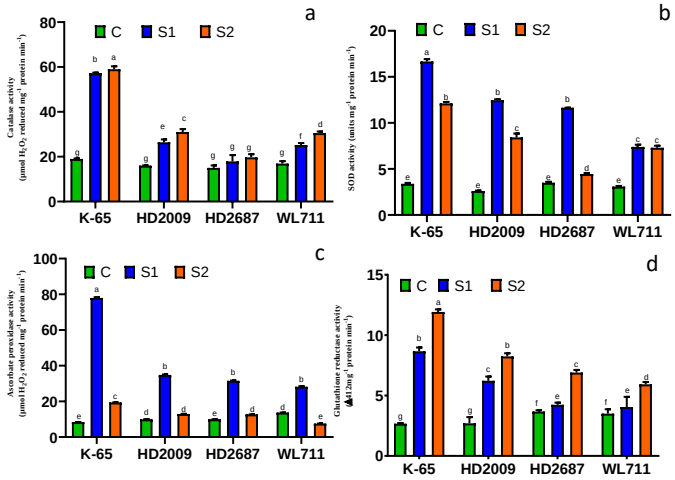

Fig. 3 Effect of salinity stress (C: control, 1.1dSm^{-1} S1: 9.1dSm^{-1}, S1: 14.2dSm^{-1}) on activity of Catalase (a), Superoxide dismutase (b), Ascorbate peroxidase (c) and Glutathione reductase (d) of leaves of wheat genotypes Kharchia 65 (K-65), HD2009, HD2687 and WL11. Salinity stress was imposed for 4 weeks as 100mM and 200mM NaCl to pot-grown seedlings 7days post germination. Average soil EC recorded at weekly intervals is shown as S1 and S2. Significant differences (*P*<0.05) between treatments are specified with different letters: Values are means (±SE) of 3 biological replicates.

Preprints (www.preprints.org) | NOT PEER-REVIEWED | Posted: 30 March 2021 doi:10.20944/preprints202103.0742.v1

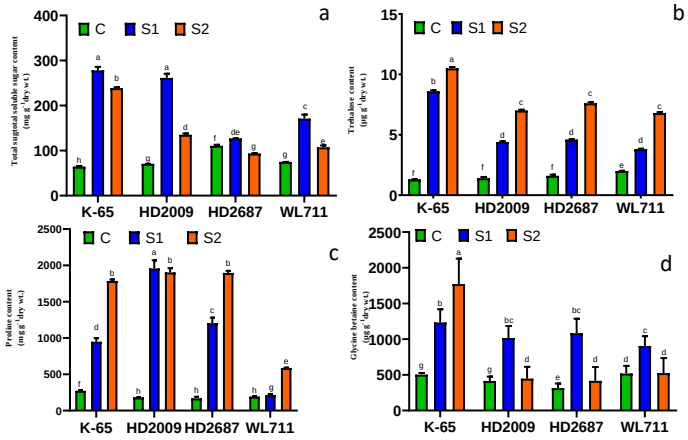

Fig. 4 Effect of salinity stress (C: control 1.1dSm^{-1} S1: 8.1dSm^{-1}, S1: 12.2dSm^{-1}) on activity of total soluble sugar (a), Trehalose (b), Proline (c) and Glycine-betaine (d) content of leaves of wheat genotypes Kharchia 65 (K-65), HD2009, HD2687 and WL11. Salinity stress was imposed for 4 weeks as 100mM and 200mM NaCl to pot-grown seedlings 7days post germination. Average soil EC recorded at weekly intervals is shown as S1 and S2. Significant differences (*P*<0.05) between treatments are specified with different letters: Values are means (±SE) of 3 biological replicates.

Preprints (www.preprints.org) | NOT PEER-REVIEWED | Posted: 30 March 2021 doi:10.20944/preprints202103.0742.v1

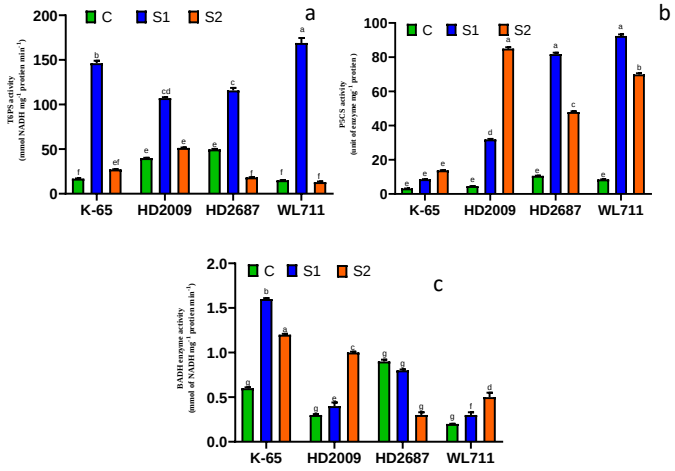

Fig. 5 Effect of salinity stress (C: control 1.1dSm^{-1} S1: 8.1dSm^{-1}, S1: 12.2dSm^{-1}) on activity of Trehalose-6-phosphate synthase (a), Pyrrolene-5-carboxylate synthase (b) Betain aldehyde dehydrogenase (c) content of leaves of wheat genotypes Kharchia 65 (K-65), HD2009, HD2687 and WL11. Salinity stress was imposed for 4 weeks as 100mM and 200mM NaCl to pot-grown seedlings 7days post germination. Average soil EC recorded at weekly intervals is shown as S1 and S2. Significant differences (*P*<0.05) between treatments are specified with different letters: Values are means (±SE) of 3 biological replicates.

Preprints (www.preprints.org) | NOT PEER-REVIEWED | Posted: 30 March 2021 doi:10.20944/preprints202103.0742.v1

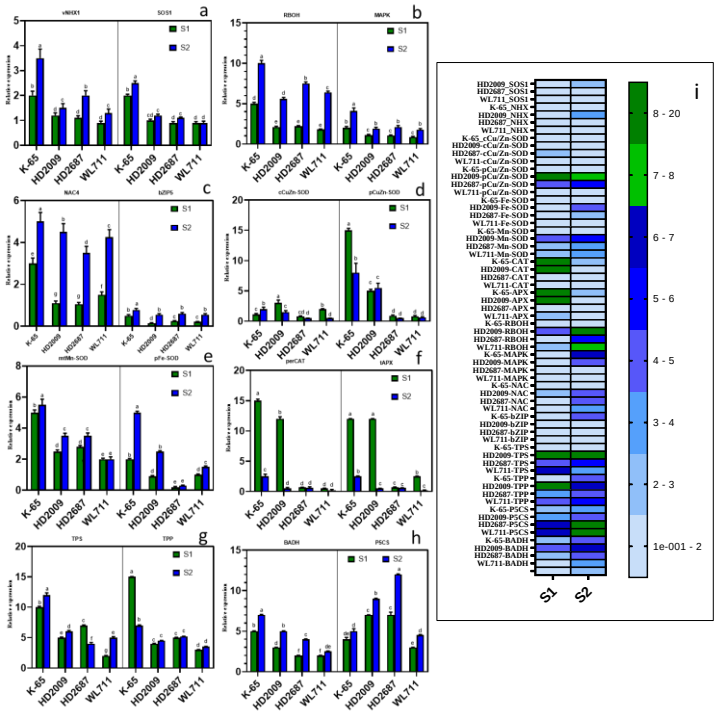

Fig. 6 Effect of salinity stress (C: control 1.1dSm^{-1} S1: 8.1dSm^{-1}, S1: 12.2dSm^{-1}) on relative expression (w.r.to control) of genes associated with tissue tolerance to salinity tolerance in leaves of wheat genotypes Kharchia 65 (K-65), HD2009, HD2687 and WL11 (a-h) and heat map depicting relative expression (i). Salinity stress was imposed for 4 weeks as 100mM and 200mM NaCl to pot-grown seedlings 7days post germination. Average soil EC recorded at weekly intervals is shown as S1 and S2. Significant differences (*P*<0.05) between treatments are specified with different letters: Values are means (±SE) of 3 biological replicates.

Preprints (www.preprints.org) | NOT PEER-REVIEWED | Posted: 30 March 2021 doi:10.20944/preprints202103.0742.v1

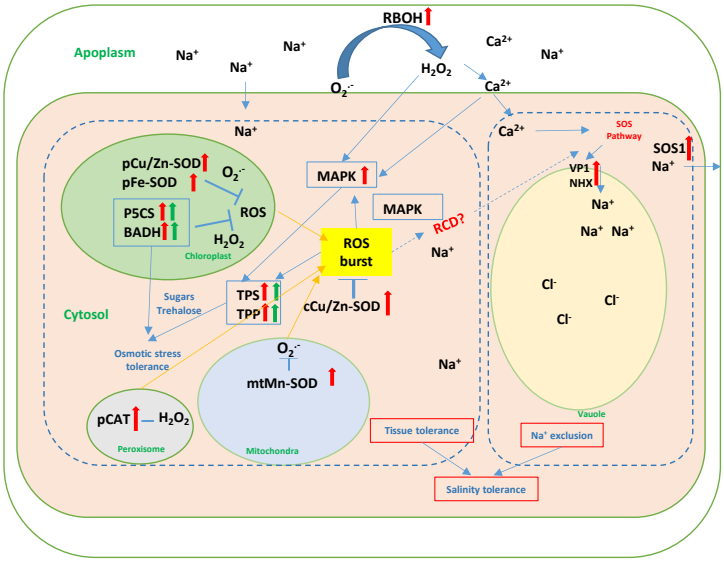

Tissue tolerance to vegetative stage salinity stress in tolerant genotype(s). Sensing of salinity stress at plasma membrane activates NADPH Oxidase (RHOH) genes and generate reactive Oxygen Species (ROS) at apoplast. Apoplastic ROS triggers calcium influx and activates calcium signaling genes of SOS pathway. ROS generated from organelles chloroplast, peroxisome and mitochondria triggers cellular oxidative burst. ROS and Calcium activates MAPK genes and downstream transcription factors , NAC and bZIP. MAPK signaling induces cellular antioxidant and compatible osmolyte biosynthesis and imparts tissue tolerance to salinity. ROS burst mediated triggering of putative RCDs and calcium signaling improves sodium exclusion and vacuolar sodium compartmentation by activating SOS1, VP1 and NHX1.